Soft Matter

Temperature Sensitive Supramolecular Self Assembly of per-6-PEO-β-cyclodextrin and α,ω-Di-(adamantylethyl)poly(N-isopropylacrylamide) in Water

V. Bennevault[abc], C. Huin[d], P. Guégan[bc*], E. V. Korchagina[e], X.-P. Qiu[e] and F. M. Winnik[efg*]

[a] Université d'Evry Val d'Essonne, 91025 Evry Cedex, France

[b] Sorbonne Universités, UPMC Université Paris 06, UMR8232, IPCM, Chimie des Polymères, 75005 Paris, France

[c] CNRS, UMR8232, IPCM, Chimie des Polymères, 75005 Paris, France

[d] Laboratoire Analyse et Modélisation pour la Biologie et l'Environnement, UMR8587 UEVE-CNRS-CEA, 91025 Evry Cedex, France

[e] Department of Chemistry and Faculty of Pharmacy, University of Montreal, CP 6128 Succursale Centre Ville, Montreal, QC, H3C3J7, Canada

[f] WPI International Center for Materials Nanoarchitectonics (MANA), National Institute for Materials Science, 1-1 Namiki, Tsukuba, Ibaraki 305-0044 Japan

[g] Department of Chemistry and Faculty of Pharmacy, University of Helsinki, Helsinki FI 00014

Abstract

The host/guest interactions in water of a star polymer consisting of a β-cyclodextrin (β-CD) core bearing six poly(polyethylene oxide) arms linked to the C_6 positions of β-CD (β-CD-PEO$_7$, M_n 5,000 g.mol^{-1}) and α,ω-di-(adamantylethyl)poly(N-isopropylacrylamide (Ad-PNIPAM-12K, M_n 12,000 g.mol^{-1}) were studied by 1D and 2D ^{1}H and ^{13}C NMR spectroscopy, isothermal calorimetry (ITC), and light scattering (LS). In cold water (T < 26 ^{o}C) supramolecular "dumbbell" assemblies, consisting of

PNIPAM chains with β-CD/Ad inclusion complexes at each end, formed via β-CD-insertion of the terminal Ads through the β-CDs secondary face. Light scattering, microcalorimetry (DSC), and DOSY NMR studies indicated that mixed aqueous solutions of β-CD-PEO$_7$ and Ad-PNIPAM-12 undergo a reversible heat-induced phase transition at ~ 32 ^{o}C, accompanied by a release of a fraction of the Ad-bound β-CD-PEO$_7$ into bulk solution and the formation of aggregated Ad-PNIPAM-12K stabilized by a β-CD-PEO$_7$ shell.

1. Introduction

The creation of polymeric supramolecular assemblies is a f ertile field of current research, generating a realm of structures, such as polymeric micelles[1,2], polymersomes[3], polyrotaxanes[4,5], hydrogels[6,7], nanotubes[8,9,10]. Applications in drug delivery[11], nanoreactors [12], or nanopores, to name but a few,[13,14] have been reported and opened new areas for materials development. Formation of reversible assemblies has been achieved through hydrogen bonding[15,16], metal coordination[17,18], arene-arene[19] (π-π), ionic,[20] and hydrophobic interactions[21]. Cyclodextrins-based inclusion complexes are used often to construct functional supramolecular assemblies through hydrophobic interactions[22]. Cyclodextrins are cyclic oligosaccharides consisting of 6, 7, or 8 glucopyranose units linked by 1,4-α-glycosidic bonds named, respectively, α, β, or γ-CD. They have a truncated conical shape with a hydrophilic outer part and a hydrophobic cavity that enables the formation of host-guest inclusion complexes that can be dissociated by application of stimuli, such as heat, addition of competitive guests or dilution.

The development of well-defined functional polymers bearing CD units, such as star polymers[23,24,25], linear polymers end-capped by CD unit(s)[26,27], or polymers with CD

pendant groups,[28] has lead to a library of new supramolecular architectures[29] with reversible topology through host/guest chemistry. Polymeric building blocks AB_2 with one adamantyl and two CD moieties at the chain ends led to the formation of hyperbranched polymers[30], while CD-based star polymers led to the formation of mikto-star[31,32], dumbbell[23,33] and H-shaped[34] copolymers. Polymers with CD pendant groups were used to generate comb polymers[28,35] and reversible networks[36,37]. Polymers end-capped with CD were employed to form block copolymers[26,38] and cyclic polymers[39]. The use of responsive polymers to construct the supramolecular structures offers new opportunities to design multi-stimulable materials as intelligent switches. The stimuli commonly used include pH[40], light[38,41], magnetic field[42], chemical[43] and temperature[23,36]. Temperature-sensitive assemblies take advantage of polymer/water systems that exhibit a lower critical solution temperature (LCST) in their phase diagram.

Poly(*N*-isopropylacrylamide) (PNIPAM) is very soluble in cold water up t o a temperature around 32 °C. At this temperature aqueous PNIPAM solutions undergo a phase transition observed macroscopically by a change of the solution appearance from clear to turbid. The phase transition is a consequence of the dehydration, collapse, and aggregation of PNIPAM chains. This process is accompanied by release of bound water into bulk, which is detected by an endotherm ($\Delta H \sim 1.4$ kcal/NIPAM unit) with a maximum $T_m \sim 32$ °C.[44] This temperature may be raised or lowered via introduction of hydrophobic/hydrophilic groups along the chain or on the chain ends[26]. Tunability of the LCST of PNIPAM is well documented and various strategies were reported to tune the LCST of PNIPAM between 26 and 34°C[45,46,47]. Heating an aqueous solution of PNIPAM leads to the formation of rigid mesoglobules, with a hydrodynamic radius of 50 to 200 nm, that resists macroscopic

phase separation[48]. The control of the mesoglobule size is achieved by control of physicochemical conditions, such as heating rate and polymer concentration[49]. To the best of our knowledge, reduction of the mesoglobule size through chemical modification has not been reported yet.

We report here the construction of supramolecular structures formed by interaction of CD-based star polymers and α,ω-di(adamantylethyl)-PNIPAM in aqueous solution. The star polymer was synthesized by "click" ligation of linear α-methoxy-ω-propargylpolyethylene oxide to per-6-deoxy-6-azido-β-cyclodextrin. The α,ω-di(adamantylethyl)-PNIPAM was synthesized by end-modification of α,ω-dithiol-PNIPAM obtained by RAFT polymerization of NIPAM. Supramolecular assemblies of the two polymers were constructed in aqueous solution and studied as a function of temperature and concentration by isothermal titration calorimetry (ITC), differential scanning calorimetry (DSC), dynamic and static light scattering (DLS and SLS), and multinuclei NMR spectroscopy. Remarkably the assemblies, which are stable at room temperature, underwent dynamic release/reinsertion of the β-CD-PEO$_7$/Ad-PNIPAM motif as a result of heating and cooling, respectively, within the 25 $^\circ$C to 50 $^\circ$C temperature range.

2. Experimental Section

2.1 Materials. All chemicals were purchased from Sigma-Aldrich chemicals Co. unless otherwise specified. Azobisisobutyronitrile (AIBN, 98%) was recrystallized from methanol prior to use. *N*-Isopropylacrylamide (NIPAM, 99%) was obtained from Acros Organics and recrystallized from an acetone/hexane (4/6, v/v) mixture. 1-Adamantaneethanol (98%), methanesulfonyl chloride (99%), sodium azide (99.5%), triphenylphosphine (98.5%), tetrabromomethane (99%), hydrated copper sulfate

(99%, Fluka), sodium ascorbate (99%, Fluka) and ammonium hydroxide solution (5M, Fluka) were used as received. Propargyl bromide was received in solution (80 wt. % in toluene) and was used without further purification. The β-cyclodextrin (98%) was purified before use. An aqueous saturated solution of β-CD was prepared at 80°C, then slowly cooled down to room temperature and let at 0°C for one night. The crystallized β-CD was then filtered and dried under vacuum at 80°C over one night. α-Methoxypolyethylene oxide was purchased from Acros Organics. 1,4-Dioxane, *N,N*-dimethylformamide (DMF) and tetrahydrofuran (THF) were purified by a solvent purification system with two packed columns of activated alumina provided by Innovative Technology Inc. All other solvents were of reagent grade and used as received. Water was deionized using a Millipore MilliQ system.

2.2 Synthesis of adamantane derivatives and polymers

1-Adamantaneethyl Iodide

1-Adamantaneethanol (1.8 g, 10 m mol) and methanesulfonyl chloride (1.7 g, 15 mmol) were dissolved in 20 mL of THF. A solution of triethylamine (1.5 g, 15 mmol) in THF (5.0 mL) was added dropwise to the stirred solution cooled in an ice-bath. At the end of the addition, the reaction solution was allowed to warm to room temperature and stirred for 5 hours. Subsequently, the solvent was removed by rotary evaporation under vacuum. The remaining light yellow liquid was dissolved in CH_2Cl_2 (5.0 mL), washed in sequence with aqueous HCl (0.5 M) solution, saturated $NaHCO_3$ solution, brine, and water. The organic phase was separated and dried over anhydrous Na_2SO_4 overnight. CH_2Cl_2 was removed by rotary evaporation. The remaining light yellow liquid was dissolved in acetone (40 mL). Sodium iodide (7.5 g, 50 mmol) was added to the solution. The mixture was stirred in the dark under N_2

atmosphere at room temperature for 2 da ys. Subsequently, the insoluble salt was removed by filtration. The solvent was evaporated in vacuum. The remaining solid was dissolved in a small amount of CH_2Cl_2 and purified by flash chromatography of silica gel using CH_2Cl_2/hexane (1:1 v:v) as eluent. Yield 2.2 g, 76%. ^{1}H NMR (CDCl$_3$) ppm, δ 1.52 (d, 6H, adamantane C-C**H**$_2$-), 1.60-1.70 (q, 6H, adamantane C-CH$_2$-CH-C**H**$_2$-), 1.80-1.84 (m, 2H, I-CH$_2$-C**H**$_2$-), 1.98 (s, 3H, adamantane C-CH$_2$-C**H**-), 3.18-3.22 (m, 2H, I-C**H**$_2$-CH$_2$-) (Figure S1).

α, ω-Di(adamantine)ethyl poly(*N*-isopropylacrylamide) (Ad-PNIPAM-12K, Scheme 1)

The precursor polymer, α,ω-dithiol poly(*N*-isopropylacrylamide) ($\overline{M_n}$ = 12,000 g/mol, as determined by GPC using DMF as eluent) was prepared by RAFT polymerization using diethylene glycol di(2-(1-isobutyl)sulfanylthiocarbonylsulfanyl-2-methyl propionate) as the chain transfer agent and subsequent aminolysis to convert the 2-(1-isobutyl)sulfanylthiocarbonylsulfanyl into thiol, as reported previously.[50] The reaction of α,ω-dithiol poly(*N*-isopropylacrylamide) with 1-adamantaneethyl iodide was carried out according to a previously reported procedure[51]. Briefly, α,ω-dithiol poly(*N*-isopropylacrylamide) (0.60 g, 0.05 mmol) and 1-adamantaneethyl iodide (44.0 mg, 0.150 mmol) were dissolved in 5 – 10 mL of DMF. A catalytic amount of the reducing agent triphenylphosphine was added to prevent the formation of disulfide bonds during reaction. The reaction mixture was stirred at room temperature under N$_2$ atmosphere overnight. The product was recovered by precipitation into diethyl ether and purified by two consecutive precipitations from THF into diethyl ether.

^{1}H NMR (CDCl$_3$) ppm, δ 1.02 (d, -CH$_2$C(C**H**$_3$)$_2$), 1.16 (s, -NHCH(C**H**$_3$)$_2$), 1.20-2.40 (multiplet, polymer backbone protons), 1.50 (s, C-C**H**$_2$- (adamantane)), 1.60-1.70 (s,

6

C-CH$_2$-CH-C**H**$_2$- (adamantane)), 1.98 (s, C-CH$_2$-C**H**- (adamantane)), 3.28 (s, -SC**H**$_2$), 3.66 (s, -OC**H**$_2$), 4.02 (s, -NHC**H**), 4.22 (s, -C(=O)OC**H**$_2$), 6.40 (bs, -C(=O)N**H**) (Figure S2).

Heptakis(6-deoxy-6-azido)β-CD (β-CD-N$_3$)

Sodium azide (6.81g, 88 mmol) was added to a solution of β-cyclodextrin (1.0 g, 0.88 mmol) in dry DMF (90 mL). The resulting suspension was stirred at 80 °C under N$_2$ for 2 hr. The reaction mixture was cooled to room temperature and treated with PPh$_3$ (6.91 g, 26.4 mmol). A freshly prepared solution of CBr$_4$ (8.76 g, 26.4 mmol) in DMF (10 mL) was rapidly added to the mixture. The orange-yellow solution was stirred at room temperature under N$_2$ for 48 hr. Methanol (5 mL) was added to quench the reaction. The product was precipitated by addition of ethanol (300 mL). It was separated by filtration and washed with ethanol followed by a 7:3 ethanol/water solution. The product was dried at 60 °C under high vacuum to yield a white powder (1.03 g, 90%)[52].

^{1}H NMR (DMSO-d6) ppm, δ:3.20 – 3.52 (m, 21H), 3.52 – 3.71 (m, 14H), 3.71 – 3.98 (m, 14H), 4.95 (d, J = 3 Hz, 7H), 5.81 (d, J = 2 Hz, 7H), 5.96 (d, J = 7 Hz, 7H) (Figure S3). ^{13}C NMR (DMSO-d6) ppm, δ: 52.33, 71.34, 73.00, 73.59, 84.20, 103.05 (Figure S4). IR spectrum : ν_{OH}= 3356 cm^{-1}, ν_{N3}= 2104 cm^{-1} (Figure S5).

α-Methoxy-ω-propargyl poly(ethylene oxide) ($\overline{M_n}$ = 550 g.mol^{-1})

A solution of propargyl bromide (80 wt. % in toluene) in excess was added dropwise to a mixture of α-methoxy polyethylene oxide (10 g, 18 mmol) and sodium hydroxide (1.44 g 36 mmol). The solution was stirred at 65 °C for 24 hr under N$_2$. It was cooled to room temperature and the solvent was evaporated. CH$_2$Cl$_2$ (100 mL) was added to the residue. The solution was washed with water (3 × 50 mL) until the pH of the

aqueous phase became neutral. The organic layer was retained and evaporated. The product obtained was dried under vacuum. ^{1}H NMR (CDCl$_3$) ppm, δ: 2,51 (s, 1H), 3,32 (s, 3H), 3,85 (m, 47H) 3,91 (s, 2H) (Figure S6); ^{13}C NMR (CDCl$_3$) ppm, δ: 57.03, 58.22, 63.22, 71.32, 72.32.

Heptakis[6-deoxy-6-(1,2,3-triazole-ω-methoxy poly(ethylene oxide)]-β-cyclodextrin (Scheme 2) (β-CD-PEO$_7$-5K)

Heptakis(6-deoxy-6-azido)β-CD (0.52 mmol) and hydrated copper sulfate (4.00 mmol) wee added to a solution of α-methoxy-ω-propargyl polyethylene oxide (4.00 mmol) in DMSO (20 mL). A freshly prepared solution of sodium ascorbate (8.2 mmol) in water was added dropwise to the solution and the resulting solution was stirred for 48 hr at room temperature. The crude product obtained after evaporation of the solvent was dissolved in CH$_2$Cl$_2$. The solution was treated with an ammonium hydroxide solution (NH$_4$OH, 5M) overnight before purification by a small silica gel column. The solvent was removed and the desired product was dried under vacuum[53].

^{1}H NMR (D$_2$O) ppm, δ: 3.39 (s, 21H), 3.42 (m, 7H), 3.64 (m, 7H), 3.71 (m, 308H), 3.95 (m,7H), 4.16 (m, 7H), 4.29 (m,7H), 4.42 (m, 7H), 4.48 (m,14H), 5.18 (d, 7H), 8.05 (s, 7H) (Figure 1); ^{13}C NMR (DMSO) ppm, δ: 51.20, 59.69, 64.76, 71.36, 84.29, 103.21, 127.28, 145.37 (Figure S7).

2.3 Instruments and methods

NMR Spectroscopy

^{1}H NMR spectra were recorded on a Bruker AMX-400 (400 MHz) instrument and chemical shifts are referenced to tetramethylsilane (TMS) (PNIPAM and adamantane derivatives) or on a Bruker AV300 spectrometer operating at 300 MHz (all other ^{1}H NMR (1-D), ^{13}C NMR spectra and DOSY experiments). For DOSY NMR

measurements, the maximum field gradient strength (56.8 G/cm) was calibrated using a homemade Plexiglas phantom inserted in a H_2O filled NMR tube and using the pulse program calibgp. The accuracy of the calibration was checked by measuring the self-diffusion coefficient of a H_2O/D_2O mixture (10 %/90 % in moles) at 25 °C[54]. The DOSY experiments were carried out using the stegp1s pulse sequence with a linear gradient of 16 steps between 2% and 95%. The mathematical treatment of the data was performed as were previously described[55]. The COSY, TOCSY, NOESY and HSQC experiments were performed on an Avance 600 MHz Bruker instrument. The temperature of the samples was controlled during all measurements. Temperature calibration between 298 K and 313 K was performed with a sample of 100% CH_3OH. Chemical shifts were referenced against an external reference containing 3-(trimethylsilyl)propionic-2,2,3,3-d4 acid sodium salt.

Gel permeation chromatography

Gel permeation chromatography (GPC) was performed with a system consisting of an Agilent 1100 isocratic pump, a set of TSK-gel α-M (particle size 13 μ, exclusion limit 1×10^7 Da for polystyrene in DMF) and a TSK-gel α-3000 (particle size 7 μ, exclusion limit 1×10^5 Da for polystyrene in DMF) (Tosoh Biosep) columns, a Dawn EOS multi-angle laser light scattering detector λ = 690 nm (Wyatt Technology Co.) and an Optilab DSP interferometric refractometer λ = 690 nm (Wyatt Technology Co.) under the following conditions: injection volume, 100 μL; flow rate, 0.5 mL/min; eluent, DMF; temperature, 40 °C. The dn/dc value of PNIPAM was determined to be 0.0738 mL/g at 690 nm in DMF at 40 °C using an Optilab DSP interferometric refractometer (Wyatt Technology Corp).

High-Sensitivity Differential Scanning Calorimetry (HS-DSC).

HS-DSC measurements were performed on a VP-DSC microcalorimeter (MicroCal Inc.) for which the cell volume was 0.52 mL and the external pressure was ca. 180 kPa. The heating rate was 1.0 °C/min in the temperature scans ranged from 10 to 70 °C. The experimental data were analyzed using the Origin-based software supplied by the manufacturer. The polymers were dissolved in water at a concentration of 1.0 g/L. The temperature of the phase transition (T_m) was taken at the maximum of the endotherm. For each experiment, three heating and cooling scans were recorded consecutively.

Isothermal Titration Calorimetry (ITC)

Isothermal titrations were performed with a MicroCal VP-ITC microcalorimeter equipped with a 1.43 mL sample cell and a 300 μL syringe. For cmc measurements, a 8.0 g/L solution of Ad-PNIPAM-12K was titrated into water in 56 aliquots (5 μL each). For the study of inclusion complex between Ad-PNIPAM-12K and β-CD/β-CD-PEO$_7$, β-CD/β-CD-PEO$_7$ solutions were loaded in the syringe and injected into the cell in 28 aliquots (10 μL each) at an interval of 300 seconds. The cell temperature was set at 20 °C in all experiments. An aqueous solution of unmodified PNIPAM was used as a blank in control experiments. The experimental data were analyzed using the Origin-based software supplied by the manufacturer.

Static and Dynamic Light Scattering Measurements (SLS and DLS)

Light scattering experiments were performed on an ALV GmbH instrument equipped with a CGS-3 goniometer and an ALV-5000 multiple digital time correlator. A He-Ne laser operating at a wavelength of $\lambda_0 = 632.8$ nm was used as the light source. All solvents and solutions were filtered through 0.22 μm pore size filter directly into the 10 mm sample cells. DLS measurements were done at a scattering angle $\theta = 90°$. The Hydrodynamic radii distribution was obtained by analysis of the correlation function

using the ALV software provided by manufacturer. For critical aggregation concentration (cac) determination, aliquots of a solution of Ad-PNIPAM-12K in water (8.0 g/L) was added stepwise into a specified amount of water placed in the sample cell to prepare solutions of increasing polymer concentration. Scattering intensities were determined at right angle and plotted against polymer concentration. The cac was determined as the crossing of the linear fits of intensities before and after the increase in scattering intensity that signals the onset of interpolymeric assembly. For DLS and SLS studies performed with solutions heated above the phase transition temperature, polymer solutions of low concentration (0.02 g/L) were used. They remained clear to the eye when heated above the polymer cloud point. Solutions were kept at 52 °C for at least 1 hr prior to measurements. The scattering angle varied from 30 to 150°. In DLS experiments relaxation time was registered at each angle. The diffusion coefficient was obtained from a plot of the relaxation rate (reciprocal relaxation time) vs the square of the scattering vector q^2 ($q = \dfrac{4\pi n}{\lambda_0} \cdot \sin(\theta/2)$), n- refractive index of water. The hydrodynamic radius was calculated using Stokes-Einstein equation[55]. In SLS experiments, the angular dependence of the excess absolute time-average scattered intensity with respect to the solvent (Rayleigh ratio R) was measured. Parabolic approximation of the plot R (q^2) was used to obtain radius of gyration R_g.

Temperature dependent measurements were done with 1 g /L solutions of Ad-PNIPAM-12K (1.0 g/L) without and with a 2 fold molar excess of β-CD or β-CD-PEO$_7$ versus adamantane (r = [β-CD]/[Ad] = 2). The temperature was increased from 15 to 50 °C, and back, with the approximate heating/cooling rate of 0.3 °C/min. Data were collected at 90 °.

3. Results

3.1 Preparation and characterisation of the polymers.

The polymer β-CD-PEO$_7$ (Scheme 2) was obtained by reaction of propargyl groups linked to one end of polyethylene oxide (PEO) chains with azide groups linked to the seven primary carbons of β-CD, as described in detail in a previous publication[53]. The Huisgen [2+3] cycloaddition between α-methoxy-ω-propargyl-PEO, synthesized by a phase transfer catalysed reaction of propargyl bromide with the ω-hydroxyl group of α-methoxy-ω-hydroxy-PEO,[57] and heptakis(6-deoxy-6-azido)-β-CD was performed in DMSO using 1.1 equivalents, with respect to the azide functions, of both CuSO$_4$.xH$_2$O and α-methoxy-ω-propargyl-PEO, in order to ensure that a PEO chain is linked to all the azide moieties of β-CD-N$_3$. The use of a polar solvent, either DMF or DMSO, significantly reduces the undesired association of Cu^{II} ions with the CD secondary face that takes place in non-polar solvents.

The success of the coupling of PEO chains to the cyclodextrin ring was confirmed by the presence of a singlet around 8.05 ppm, assigned to the triazole proton (H7), in the ^{1}H NMR spectrum of β-CD-PEO$_7$ in D$_2$O (Figure 1). This spectrum also presents signals due to the cyclodextrin ring protons (from ~ 3.3 to 5.3 ppm), a singlet at 3.39 ppm assigned to the terminal methoxy group of the PEO chains, and a strong signal at 3.71 ppm due to the methylene protons of the PEO chains. The HSQC spectrum of β-CD-PEO$_7$ (Figure 2a) allows the assignments of the signals at 4.29 ppm and 4.42 ppm to the non-equivalent protons H6 and H6', respectively. Similarly, the signal at 4.48 ppm is readily assigned to the proton H8. Complete assignment of the signals in the ^{1}H NMR spectrum of β-CD-PEO$_7$ was achieved via COSY and NOESY experiments. The COSY spectrum, presented in Figure 2b, allows assignment of the

12

signals due to the protons H1 to H5 of cyclodextrin, as follows: H1 (5.18 ppm), H2 (3.63 ppm), H3 (4.01 ppm), H4 (3.43 ppm) and H5 (4.27 ppm). A TOCSY experiment was carried out in order to confirm the assignments of all CD protons (Figure S8). The NOESY spectrum (Figure 3) shows that the triazole proton (H7) is correlated via a n egative cross-peak to H1, H2, H3, H4, H5, H6, H6'and H8. We confirmed that the assignments obtained via 2D NMR spectroscopy agree well with the integration of the signals in the 1D NMR spectrum of β-CD-PEO$_7$.

α,ω-Di-(adamantylethyl)-poly(N-isopropylacrylamide)   (Ad-PNIPAM-12K)   was prepared by nucleophilic substitution of the mercaptan functions linked to each end of the PNIPAM chains with iodoethyladamantane (Scheme 1), following a procedure reported earlier for the preparation of α,ω-dipyrenyl- and α,ω-dicholesteryl-PNIPAM[50]. The level of functionalization, assessed by the Ellman test for residual thiols[58] was greater than 90 %. The ^{1}H NMR spectrum of Ad-PNIPAM-12K in CDCl$_3$ (Figure S2), displayed signals characteristic of PNIPAM, as well as signals at 1.50 and 1.98 ppm ascribed, respectively, to the resonances of the protons -C-C*H*$_2$- and -C-CH$_2$-C*H*- of the adamantyl end groups.

3.2 Properties of β-CD-PEO$_7$ and Ad-PNIPAM-12K in water. The polymer β-CD-PEO$_7$ readily dissolves in water at all temperatures within the range of interest in this study (~ 5 ^{o}C to ~ 80 ^{o}C), up to a concentration of ~ 22 g/L. Above this concentration, intermolecular association of β-CD-PEO$_7$ occurs. Ad-PNIPAM-12K is soluble in cold water. When the polymer concentration exceeds ~ 0.25 g/L or ~ [Ad] ~ 4×10^{-5} mol/L, the chains aggregate as seen by an increase in the intensity of the light scattered by the solution (Figure 4a), DLS studies indicate that nanoparticles of hydrodynamic radius R$_h$~30 nm coexist with Ad-PNIPAM-12K unimers, (Figure 5a, black squares). The concentration range over which aggregation takes place was determined also by

isothermal titration calorimetry (ITC) which monitors the heat exchange upon titration of an aqueous solution of Ad-PNIPAM-12K (8.0 g/L) into water (Figure 4b). Aqueous solutions of Ad-PNIPAM-12K undergo a phase transition upon heating. The transition temperature recorded by HS-DSC (Figure S9) is T_m = 27.4 ^{o}C. This temperature is lower than the value recorded in the case of the unmodified PNIPAM sample of identical molar mass (33.5 °C)[59]. The decrease of the phase transition temperature upon end-modification of PNIPAM with adamantylethyl groups can be attributed to the hydrophobic nature of the adamantylethyl end-groups, as reported in the case of other alkyl or aryl-end modified PNIPAMs[60].

3.3 Interactions between β-CD-PEO$_7$ and Ad-PNIPAM-12K in water below the phase transition temperature of Ad-PNIPAM-12K.

Simple visual observation of Ad-PNIPAM-12K solutions before and after addition of β-CD suggests that the end-groups of Ad-PNIPAM-12K are able to form inclusion complexes with β-CD. In the top right section of Figure 5, we present photographs of vials kept at room temperature (20 ^{o}C) containing an aqueous solution of Ad-PNIPAM-12K (5 g.L^{-1}) alone (left) and in the presence of either β-CD (middle) or β-CD-PEO$_7$ (right) with [Ad]:[β-CD]=1:2 in both cases ([Ad] and [β-CD] represent respectively the concentration of adamantyl and β-CD groups). The Ad-PNIPAM-12K solution is slightly turbid, due to the formation of Ad-PNIPAM-12K aggregates. Upon addition of β-CD or β-CD-PEO$_7$ in an amount such that [Ad]:[β-CD]=1:2, the solution becomes clear, which can be taken as an indication that the Ad-PNIPAM-12K aggregates are destroyed by β-CD or β-CD-PEO$_7$. Inclusion of Ad into the hydrophilic β-CD presumably increases the solubility of Ad-PNIPAM-12K in water.

14

Isothermal Titration Calorimetry (ITC)

Isothermal titrations were carried out by adding solutions of β-CD (3.6 mmol) or β-CD-PEO$_7$ (4.0 mmol of β-CD) to an Ad-PNIPAM-12K solution (0.33 mmol of Ad). Titrations of β-CD and β-CD-PEO$_7$ into PNIPAM were carried out under the same conditions (Figure S10). The resulting enthalpograms were subtracted from the corresponding titrations of Ad-PNIPAM-12K in order to remove heat effects associated with the dilution of β-CD and β-CD-PEO$_7$ and possible interactions of the titrants with the PNIPAM backbone. Figure 5c depicts the enthalpogram of β-CD into Ad-PNIPAM-12K. The curve was fitted to a one binding site model that led to a ~ 1:1 Ad/β-CD ratio and an association constant of 1.3×10^5 L.mol^{-1}, a value typical for the association between adamantyl derivatives and β-CD[35,61]. The enthalpogram corresponding to the titration of β-CD-PEO$_7$ into Ad-PNIPAM-12K is presented in Figure 5d. A fit to a one-binding site model gave a binding constant of 2.4×10^4 L.mol^{-1}, a value significantly lower than the association between Ad-PNIPAM-12K and β-CD, in agreement with previous reports on t he binding of adamantyl derivatives to polymer-bound β-CD[35,61].

Dynamic light scattering measurements

Having established the formation of inclusion complexes between the end-groups of Ad-PNIPAM-12K (guests) and β-CD-PEO$_7$, we set about to assess the consequences of the complexation on t he solution properties of Ad-PNIPAM-12K. DLS measurements performed for mixed solutions of Ad-PNIPAM-12K and either β-CD-PEO$_7$ or β-CD (Figure 5a) indicated that when the molar ratio r = [CD]/[Ad] is equal to 2, the contribution of Ad-PNIPAM-12K aggregates to the scattering intensity is significantly reduced and that scattering objects of $R_h \sim 3$ nm become predominant.

The latter are attributed tentatively to isolated Ad-PNIPAM-12K chains carrying β-CD groups associated to the adamantyl end groups.

1D and 2D NMR measurements

The stoechiometry of the Ad-PNIPAM-12K/β-CD-PEO$_7$ complex in mixed systems of varying adamantyl to β-CD molar ratio was investigated by ^{1}H NMR spectroscopy. Spectra of mixed solutions ([Ad-PNIPAM-12K]=$2.50.10^{-3}$ mol.L^{-1}; [β-CD-PEO$_7$]=$1.25.10^{-3}$ to $6.25.10^{-3}$ mol.L^{-1}) kept at 23°C (r = [CD]/[Ad] ranging from 0.25 to 1.25) were recorded and compared to the spectrum of β-CD-PEO$_7$. The changes of the chemical shift of the signal around 8.0 - 8.1 ppm attributed to the triazole proton are presented in Figure 6. The chemical shift of the triazole proton remained constant for 0.25 < r ≤ 1.0. However, in the spectra of solutions with r >1.0, it underwent a downfield shift, suggesting the formation of 1:1 Ad/CD inclusion complexes. The chemical shift of the CD anomeric protons at 5.17 ppm underwent a similar shift (data not shown), while the chemical shifts of the other protons on the CD groups remained constant for all solutions. These results suggest that all the CD groups form complexes with Ad as long as CD is the minority component.

A mixed solution of ratio r = 1 was analyzed by 2D NMR spectroscopy. The chemical shifts of the β-CD-PEO$_7$ protons in the presence of Ad-PNIPAM-12K were assigned as follows: H1 (5.17 ppm), H2 (3.64 ppm), H3 (3.95 ppm), H4 (3.42 ppm) and H5 (4.16 ppm) based on the TOCSY spectrum of the mixed solution. The signals due to H3 and H5, which are located inside the CD cavity, underwent an upfield shift compared to uncomplexed β-CD-PEO$_7$ [H3 (4.01 ppm); H5 (4.27 ppm)], whereas the chemical shifts of the protons H2 and H4 remained identical to those of uncomplexed β-CD-PEO$_7$. This observation confirms that the adamantyl moiety is located within

16

the hydrophobic CD cavity. The NOESY NMR spectrum of mixed solution (Figure 7) exhibited intense correlation peaks between H3 and H5 and the protons linked to the adamantyl group. The latter signals, which are masked by the signals due to the C*H*-CO and C*H*$_2$ protons of the polymer backbone in the ^{1}H NMR spectrum of the mixed solution, are readily identified by a negative cross-peak in the 2D spectrum. The NOESY spectrum gave the following chemical shifts: 1.65 ppm, 1.80 ppm, 1.96 ppm and 2.25 ppm which were assigned to the residue -CH$_2$-Ad (Figure 7). Moreover, it was noted that the intensity of the signals correlation peaks is higher for H3 than H5, implying that the inclusion of Ad into CD occurred mainly via the CD secondary rim, in agreement with Carrazana *et al*[58]. The steric hindrance induced by the PEO chains linked to the primary rim further enhances the preferred entry of CD via the secondary rim.

Diffusion-ordered spectroscopy (DOSY) NMR experiments, which are based on a pulse-field gradient spin-echo NMR measurements on m ixtures of diffusing components[62-65] were performed as well, using solutions of β-CD-PEO$_7$ concentration lower than the polymer cac, with r = 1: [Ad-PNIPAM-12K] = 0.5×[β-CD-PEO$_7$] = 3.125×10^{-4} mol.L^{-1}. The diffusion coefficients recorded at 23°C are presented in Table 1. In this mixture, Ad-PNIPAM-12K and β-CD-PEO$_7$ have similar diffusion coefficients, bringing further evidence of the Ad/β-CD complexation linking the two polymers.

3.4 Temperature-dependence of the interactions between β-CD-PEO$_7$ and Ad-PNIPAM-12K in water

As presented in Figure 8, left, aqueous solutions of Ad-PNIPAM-12K are slightly turbid at room temperature, whereas mixed solutions of Ad-PNIPAM-12K and either

17

β-CD or β-CD-PEO$_7$ are clear as a consequence of the β-CD-induced disruption of Ad-PNIPAM-12k aggregates. Solutions of Ad-PNIPAM-12K with or without β-CD or β-CD-PEO$_7$ became cloudy upon heating to 50 ^{o}C (Figure 8, right). Upon cooling to room temperature, the samples recovered their original appearance. This observation is quite important, since it implies that the major amount of Ad/β-CD inclusion complexes are broken during the heat treatment, but they form again upon cooling. The experiments described below were performed in order to get a firmer description of the response of mixed systems to changes in temperature.

HS-DSC measurements

First, the phase transition of Ad-PNIPAM-12K in mixed aqueous solutions of either β-CD-PEO$_7$ or β-CD (r = 1 and r = 2) was examined by HS-DSC measurements. In the presence of β-CD-PEO$_7$ the temperature corresponding to the endotherm maximum (T$_m$) increased from 27.4°C (no added β-CD-PEO$_7$) to 30.1°C (r = 1) and 31.1°C (r =2), while in the presence of β-CD the T$_m$ value shifted from 27.4°C to 31.9°C (r = 1) and 33.3 °C (r = 2). The corresponding endotherms are presented in Figure S9 and S11. The enthalpy of the transition was also affected by the presence of β-CD-PEO$_7$ or β-CD. It increased from 1.42 ± 0.10 kcal/mol^{-1} (Ad-PNIPAM-12K alone) to 1.56 ± 0.12 kcal/mol^{-1} (r = 1) and 1.67 ± 0.12 kcal/mol^{-1} (r = 2). In order to understand the changes in the transition enthalpy, it is important to compare first the transition enthalpy for solutions of Ad-PNIPAM-12K alone to that of unmodified PNIPAM of similar molar mass (1.58 kcal.mol^{-1})[59]. The decrease of the transition enthalpy of Ad-PNIPAM-12K, compared to unmodified PNIPAM is a consequence of the steric constraints imposed by the association of Ad-PNIPAM-12K that prevent full hydration of the PNIPAM chains in the aggregates, as observed also in the case of

α,ω-di(n-octadecyl)-PNIPAM[59]. The fact that the transition enthalpy in mixed solutions of r = 2 is nearly identical to that of unmodified PNIPAM, implies that the hydration of the PNIPAM chain in solutions of cyclodextrin-capped Ad-PNIPAM-12K is similar to that of unmodified PNIPAM. Hence, the increase in the transition enthalpy of Ad-PNIPAM-12K in the presence of β-CD can be attributed to the disruption of the Ad-PNIPAM-12K aggregates that exist in cold solutions upon inclusion of the Ad endgroups into β-CD.

Light scattering measurements

DLS and SLS measurements were carried out for mixed solutions of Ad-PNIPAM-12K and β-CD or β-CD-PEO$_7$ of constant r value (r = 2) for polymer concentration c-0.02 g/L at 52 °C (Figure 9). The R_g/R_h ratios of Ad-PNIPAM-12K was 0.75 (Figure 9), a value typical for hard sphere aggregates, or mesoglobules. In mixed solutions of Ad-PNIPAM-12K/β-CD and Ad-PNIPAM-12K/β-CD-PEO$_7$ (with [Ad-PNIPAM-12]=0.02 g/L) the ratio of R_g/R_h shifts to slightly lower values, 0.65 and 0.62 (Figure 9), respectively, usually attributed to aggregates of core/shell structures. This observation may imply that a hydrophilic layer consisting of β-CD-complexed with Ad moieties forms at the periphery of the mesoglobules.

Finally, the R_h of the supramolecular dumbbell-shaped compound was measured at 52°C with r = 2, as a function of concentration ranging in concentration Ad-PNIPAM-12K from 0.0025 g/L to 0.04 g/L (Figure 10). We assume that under such conditions solutions are sufficiently diluted and any changes of the size of the collapsed aggregates are caused predominantly to their real growth upon i ncreasing the concentration. Thus way upon heating past the phase transition temperature Ad-PNIPAM-12k formed aggregates of R_h ranging from 33 nm (0.0025 g/L of Ad-

PNIPAM-12K) to 75 nm (0.04 g/L of Ad-PNIPAM-12K). It is clearly observed that the hydrodynamic radius of the aggregated supramolecular assembly is increasing with its concentration, and seems to level off at a concentration close to 0.04 g.mol^{-1}. The preparation concentration is then a stimulus that allows to adjust the size of the aggregate in the range 30 to 80 nm.

NMR experiments

1D ^{1}H NMR spectra of Ad-PNIPAM-12K and a mixed solution of Ad-PNIPAM-12K and of β-CD-PEO$_7$ (r = 1) were recorded as a function of increasing temperature using 3-(trimethylsilyl)propionic-2,2,3,3-d4 acid sodium salt as an external reference. The area of the signals between 0.6 and 2.5 ppm , attributed solely to PNIPAM, decreased abruptly with increasing temperature between 22°C and 40°C. The transition mid-points were 26°C in the case of Ad-PNIPAM-12K and 32.5°C in the mixed solution, which are values similar to the T$_m$ values recorded by HS-DSC. The small discrepancies observed may be attributed to differences in solution concentration or to the well-know effect of substituting D$_2$O for H$_2$O^{44}.

The diffusion coefficient of the Ad-PNIPAM-12K/β-CD-PEO$_7$ complex in mixed solutions r = 1 heated to 39°C was evaluated by DOSY experiments (Table 1). The diffusion coefficient of β-CD-PEO$_7$ in the mixed solution increased from 7.6×10^{-11} m^2/s (23°C) to 1.6×10^{-10} (39°C), while the Ad-PNIPAM-12K diffusion coefficient increased slightly, from 6.1×10^{-11} m^2/s (23°C) to 7.7×10^{-11} m^2/s (39°C). The diffusion coefficient of β-CD-PEO$_7$ in this solution is nearly identical to that of free β-CD-PEO$_7$ (1.7×10^{-10} m^2/s) recorded with a solution heated to 39°C. Hence, during the phase transition of the mixed solution, most of the β-CD-PEO$_7$ is expelled into bulk water, indicating the lability of the Ad/CD inclusion complex and the preferred

solubilization of Ad into the PNIPAM-rich phase formed above T_m. From LS experiments, we concluded that the Ad-PNIPAM-12K aggregates formed above T_m are surrounded by a layer of bound β-CD-PEO$_7$. The fraction of bound β-CD-PEO$_7$, compared to the β-CD-PEO$_7$ released in bulk water must be too weak for detection via DOSY measurements. All these results are reversible when decreasing the temperature. To conclude, the NMR experiments allowed to characterize the behavior of the self-assembly of Ad-PNIPAM-12K and β-CD-PEO$_7$ in function of the temperature.

4. Conclusion

The interactions at play in aqueous solutions of Ad-PNIPAM-12K and β-CD-PEO$_7$ below and above the phase transition temperature are depicted in Scheme 3. In very dilute solutions, Ad-PNIPAM-12K and β-CD-PEO$_7$ are kept apart. As the temperature increases, the two polymers behave independently and Ad-PNIPAM-12K aggregates form above the phase transition temperature, whereas β-CD-PEO$_7$ remains in water. As the concentrations of β-CD-PEO$_7$ and Ad-PNIPAM-12K increase, the inclusion complexes form between the β-CD cores of the star polymer and the adamantyl groups borne by PNIPAM, in equilibrium with polymers. Heating the solution leads to the formation of mesoglobules consisting of a core of aggregated Ad-PNIPAM-12K collapsed chains surrounded by a β-CD-PEO$_7$ shell and the release in bulk of unbound β-CD-PEO$_7$. In solutions of higher Ad-PNIPAM-12K and β-CD-PEO$_7$ concentrations, the mesoglobules formed above the phase transition increase in size and further release of β-CD-PEO$_7$ occurs. All the phenomena are reversible, suggesting possible applications of the β-CD-PEO$_7$/Ad-PNIPAM-12K supramolecular systems as temperature-driven actuators.

References

1 G. S. Kwon and T. Okano, *Advanced Drug delivery Review* 1996, **21**, Issue 2, 107-116.

2 K. Kataoka, A. Harada and Y. Nagasaki, *Advanced Drug delivery Review* 2001, **47**, Issue 1, 113-131.

3 B. M. Discher, Y. Y Won, D. S. Ege, J. C. M Lee, S. F. Bates, D. E. Discher and D. A. Hammer, *Science* 1999, **284**, n°5417, 1143-1146.

4 A. Harada, J. Li and M. Kamachi, *Nature* 1992, **356**, 325 – 327.

5 N. Jarroux, P. Guégan, H. Cheradame and L. Auvray *J. Phys. Chem. B* 2005**, 109**, 23816-23822.

6   J. Li, X. Li, Z. Zhou, X. Ni and K. W. Leong, *Macromolecules* 2001, **34** (21), 7236–7237.

7   A. Sandier, W. Brown, H. Mays and C. Amiel, *Langmuir*, 2000, **16** (4), 1634–1642.

8 A. Harada, J. Li and M. Kamachi, *Nature* 1993, **394**, 516-518.

9   H. Fenneri, B. L. Deng, A. E. Ribbe, K. Hallenga, J. Jacob and P. Thiyagarajan *PNAS* 2002, **99** (2) 6487-6492.

10 J. Couet and M. Biesalski, *Soft Matter* 2006, **2**, 1005-1014.

11 F. Yhaya, S. Binauld, Y. Kim and M. H. Stenzel, *Macromol. Rapid Commun.* 2012, **33**, 1868-1874.

12 C. De Vocht, A. Ranquin, R. Willaert, J. A. Van Ginderachter, T. Vanhaecke, V. Rogiers, W. Versées, P. Van Gelder and J. Steyaert, *Journal of Controlled Released* 2009, **137**, 246-254.

13 N. Sakai and S. Matile, *J. Am. Chem. Soc.* 2003, **125** (47), 14348-14356.

14 N. Badi, L. Auvray and P. Guégan, *Advanced Materials* 2009**, 21**, 4054-4057.

15 L. Brunsveld, B. J. B. Folmer, E. W. Meijer and R. P. Sijbesma, *Chem. Rev.* 2001, **101**, 4071-4098.

16 M. Bellot and L. Bouteiller, *Langmuir* 2008, **24** (24), 14176-14182.

17 B. G. G. Lohmeijer and U. S. Schubert, *J. of Polymer Science: part A: Polymer Chemistry* 2003, **41**, 1413-1427.

18 K. J. Calzia, G. N. Tew, *Macromolecules* 2002, **35**, 6090-6093.

19 L. Fang, S. Basu, C-H Sue, A. C. Fahrenbach and J. F. Stoddart, *J. Am. Chem. Soc*. 2011, **133**, 396–399.

20 C. F. J. Faul and M. Antonietti, *Advanced Materials* 2003, **15**(9), 673-683.

21 S. A. Nepogodiev and J. F. Stoddart, *Chem. Rev.* 1998**, 98***,* 1959-1976.

22 G. Wenz, B. H. Han and A. Müller, *Chem. Rev*. 2006, **106**, 782-817.

23 Z-X. Zhang, K. L. Liu and J. Li, *Macromolecules* 2011, **44**, 1182-1193.

24 C. Yang, H. Li, S. H. Goh and J. Li, *Biomaterials* 2007, **28**, 3245-3254.

25 K. Ohno, B. Wong and D. M. Haddleton, *J. Polym. Sci. Part A: Polym Chem* 2001, **39**, 2206-2214.

26 J. Stadermann, H. Komber, M. Erber, F. Däbritz, H. Ritter and B. Voit, *Macromolecules* 2011, **44**, 3250-3259.

27 J. Zeng, K. Shi, Y. Zhang, X. Sun and B. Zhang, *Chem. Commun.*, 2008, 3753-3755.

28 A. Bertrand, M. Stenzel, E. Fleury and J. Bernard, *Polym. Chem* 2012, **3**, 377-383.

29 F. Yhaya, A. M. Gregory and M. H. Stenzel, *Aust. J. Chem.* 2010, **63,** 195–210.

30 Z. Ge, H. Liu, Y. Zhang and S. Liu, *Macromol. Rapid Commun*. 2011, **32**, 68-73.

31 B. V. K. J. Schmidt, M. Hetzer, H. Ritter and C. Barner-Kowollik, *Polym. Chem* 2012, **3**, 3064-3067.

32 X. Huan, D. Wang, R. Dong, C. Tu, B. Zhu, D. Yan and X. Zhu, *Macromolecules* 2012, **45**, 5941-5947.

33 Z-X. Zhang, X. Liu, F. J. Xu, X. J. Loh, E-T. Kang, K-G. Neoh and J. Li, *Macromolecules* 2008, **41**, 5967-5970.

34 B. V. K. J. Schmidt and C. Barner-Kowollik, *Polym. Chem* 2014, **5**, 2461-2472.

35 C. Moers, L. Nuhn, M. Wissel, R. Stangenberg, M. Mondeshki, E. Berger-Nicoletti, A. Thomas, D. Schaeffel, K. Koynov, M. Klapper, R. Zentel and H. Frey, *Macromolecules* 2013, **46**, 9544-9553.

36 L. Li, X. Guo, J. Wang, P. Liu, R. K. Prud'homme, B. L. May and S. F. Lincoln, *Macromolecules* 2008, **41**, 8677-8681.

37 M. Hetzer, B. V. K. J. Schmidt, C. Barner-Kowollik and H. Ritter, *Polym. Chem.* 2014, **5**, 2142-2152.

38 B. V. K. J. Schmidt, M. Hetzer, H. Ritter and C. Barner-Kowollik, *Macromolecules* 2013, **46**, 1054-1065.

39 Y. Inoue, P. Kuad, Y. Okumura, Y. Takashima, H. Yamaguchi and A. Harada, *J. Am. Chem. Soc.* 2007, **129**, 6396-6397.

40 H. S. Choi, K. M. Huh, T. Ooya, N. Yui, *J. Am. Chem. Soc.* 2003, **125**, 6350-6351.

41 G. Pouliquen, C. Amiel and C. Tribet, *J. Phys. Chem. B* 2007, **111**, 5587-5595.

42 K. Lee, K. H. Bae, Y. Lee, S. H. Lee, C-H. Ahn and T. G. Park, *Macromol. Biosci*. 2010, **10**, 239–245.

43 W. Deng, H. Yamaguchi, Y. Takashima and A. Harada, *Angew. Chem*. 2007, **119**, 5236 –5239.

44 P. Kujawa and F. M. Winnik, *Macromolecules*, 2001, **34**, 4130-4135.

45 S. Dai, P. Ravi and K. C. Tam, *Soft Matter*, 2009, **5**, 2513–2533.

46 J. E. Chung, M. Yokoyama, T. Aoyagi, Y. Sakurai and T. Okano, *J Controlled Release*, 1998, **53**, 119–130.

47 Y. Xia, N. A. D. Burke and H. D. H. Stöver, *Macromolecules*, 2006, **39**, 2275–2283.

48 V. Aseyev, H. Tenhu and F. M. Winnik, *Adv. Pol. Sci*, 2011, **242**, 29-89.

49 P. Kujawa, V. Aseyev, H. Tenhu and F. M. Winnik, *Macromolecules* 2006, **39**, 7686-7693.

50 X. P. Qiu and F. M. Winnik, *Macromolecules* 2007, **40**, 872-878.

51 F. Segui, X. P. Qiu and F. M. Winnik, *J. Polym. Sci., Part A: Polym. Chem.* 2008, **46**, 314–326.

52 S. Nag, L. Duarte, E. Bertrand, V. Celton, M. Castro, V. Choudhary, P. Guegan and J-F Feller, *J. Mater. Chem. B* 2014, **2**, 6571–6579.

53 Y. El Ghoul, R. Renia, I. Faye, S. Rassou, N. Badi, V. Bennevault-Celton, C. Huin and P. Guégan, *Chem. Commun.* 2013, **49**, 11647-11649.

54 M. Holz and H. Weingärtner, *J. Magn. Reson* 1991, **92**, 115-125.

55 V. Bennevault-Celton, A. Urbach, O. Martin, C. Pichon, P. Guégan and P. Midoux, *Bioconjugate Chem*. 2011, **22**, 2404-2414.

56   W. Schartl, *Light Scattering from Polymer Solutions and Particle Dispersions*, Springer Verlag Berlin and Heidelberg, Germany, 2007, p. 18.

57   L. Lestel, P. Guégan, S. Boileau and F. Lauprêtre, *Macromolecules* 1992, **25**, 6024-6028.

58   J. Carrazana, A. Jover, F. Meijide, V. H. Soto and J. V. Tato, *J. Phys. Chem. B* 2005**, 109**, 9719-9726.

59   X. P. Qiu, T. Koga, F. Tanaka and F. M. Winnik, *Sci. China Chem.* 2013, **56**, n°1, 56-64.

60   P. Kujawa, F. Segui, S. Shaban, C. Diab, Y. Okada, F. Tanaka and F. M. Winnik *Macromolecules*, 2006, **39**, 341-348.

61   M. Othman, K. Bouchemal, P. Couvreur and R. Gref, *Int. J. Pharm.* 2009**, 379**, 218–225.

62   D. Li, G. Kagan, R. Hopson and P. G. Williard, *J. Am. Chem. Soc.* 2009**, 131**, 5627-5634.

63   S. Viel, D. Capitani, L. Mannina and A. Segre, *Biomacromolecules* 2003**, 4**, 1843-1847.

64   T. Zhao and H. W. Beckham, *Macromolecules* 2003**, 36**, 4833-4837.

65   Y. J. Wang, H. Therien-Aubin, W. E. Baille, J. T. Luo and X. X. Zhu, *Polymer* 2010**, 51**, 2345-2350.

Figures, Scheme and Tables
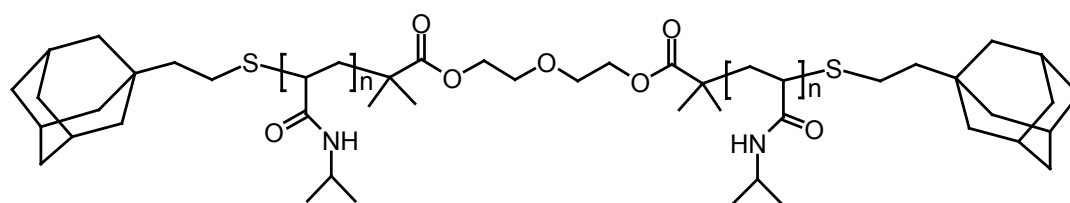
Scheme 1. Structure of Ad-PNIPAM-12K.
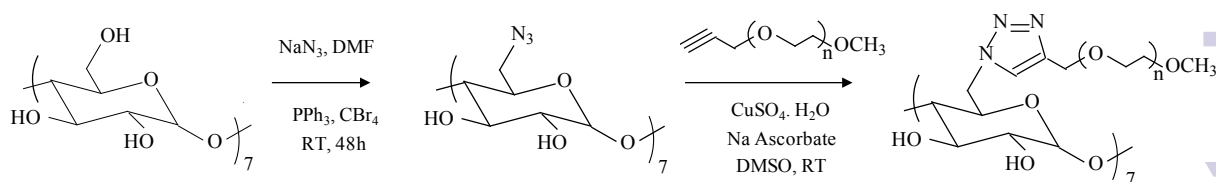
Scheme 2. Synthesis of heptakis[6-deoxy-6-(1,2,3-triazole-ω-methoxy poly(ethylene oxide))]-β-CD (β-CD-PEO$_7$)
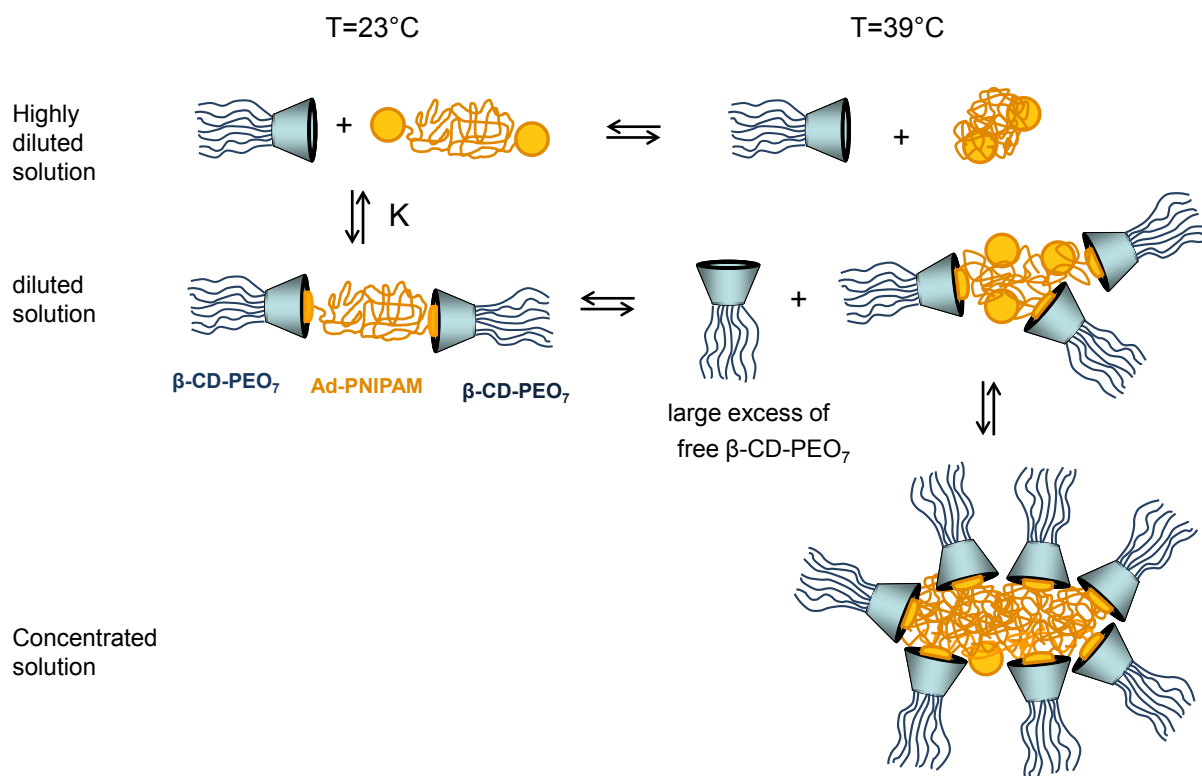
Scheme 3 : Illustration of the self-association of the Ad-PNIPAM-12K and β-CD-PEO$_7$ mixture upon changes of concentration and temperature
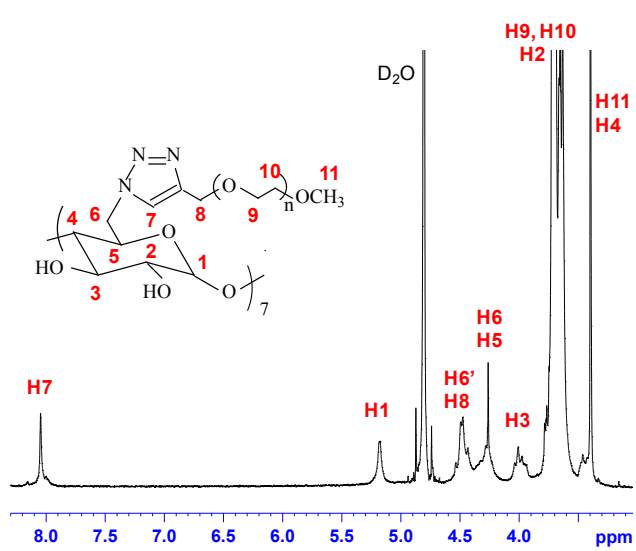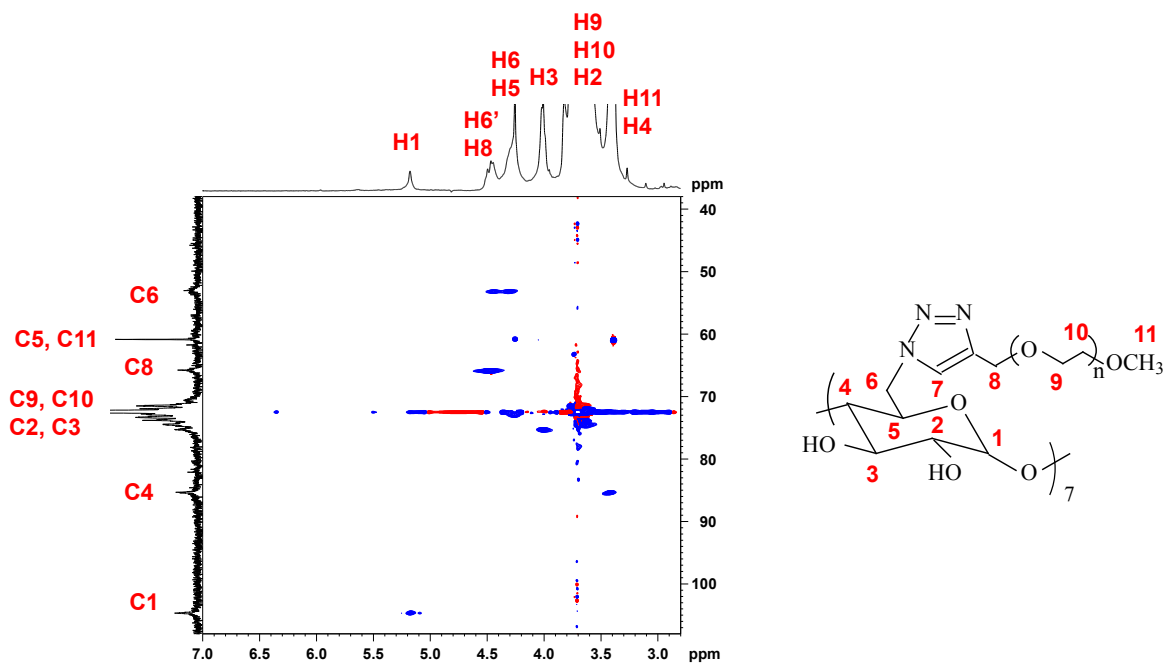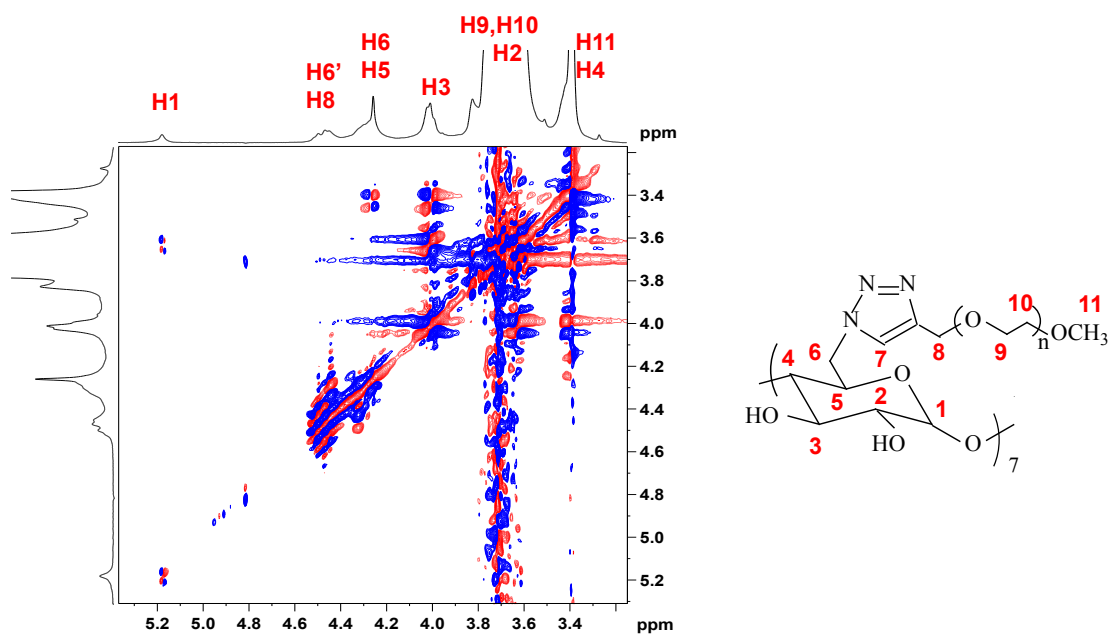

Figure 1: ^{1}H NMR spectrum of feptakis[6-deoxy-6-(1,2,3-triazole-ω-methoxy poly(ethylene oxide)]-β-cyclodextrin in D$_2$O; [β-CD-PEO$_7$]=6.25×10^{-4} mol/L

Soft Matter Accepted Manuscript

(2a)

(2b)

Figure 2: HSQC spectrum (Fig 2a) and COSY spectrum (Fig 2b) of β-CD-PEO$_7$ in D$_2$O at 25°C; [β-CD-PEO$_7$]=6.25×10^{-4} mol/L
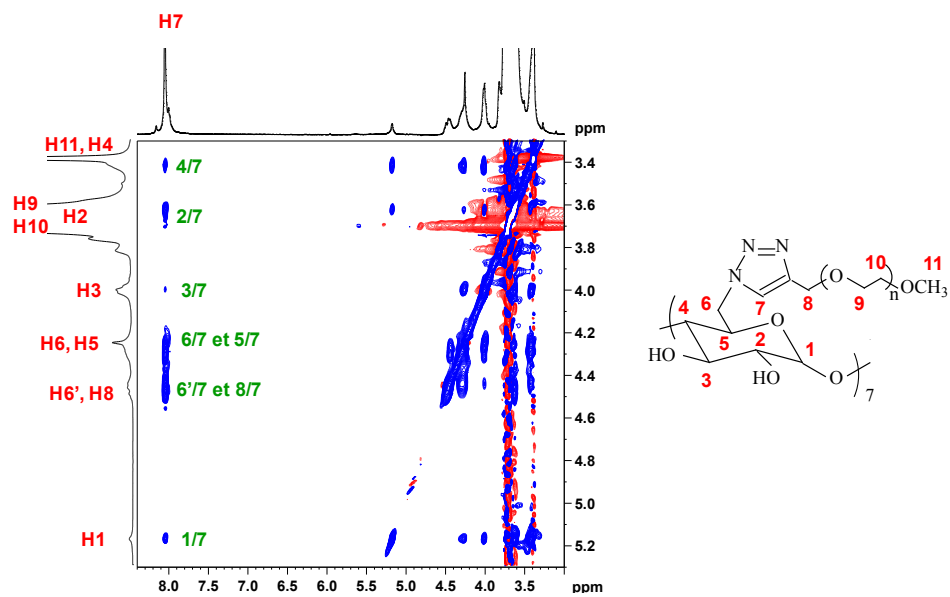
Figure 3: NOESY spectrum of β-CD-PEO$_7$ in D$_2$O at 25°C; [β-CD-PEO$_7$] = 6.25×10$^-$^{4} mol/L.
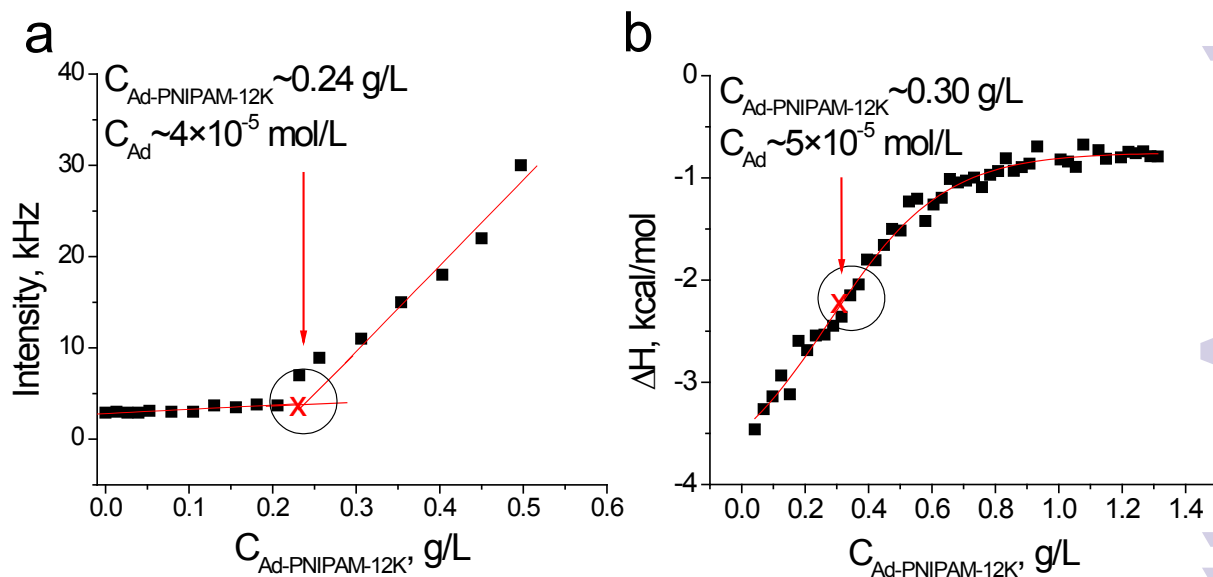
Figure 4: (a) Plot of the scattering intensity measured by SLS as a function of the concentration of Ad-PNIPAM-12K in water; temperature: 20 °C; the arrow points to the polymer concentration corresponding to the onset of aggregation; (b) Plot of the changes of the enthalpy of dilution (ΔH) of Ad-PNIPAM-12 K (8.0 g/L) into water;

temperature: 20 °C. The concentration corresponding to the mid-point of the sigmoidal curve is indicated by the arrow.
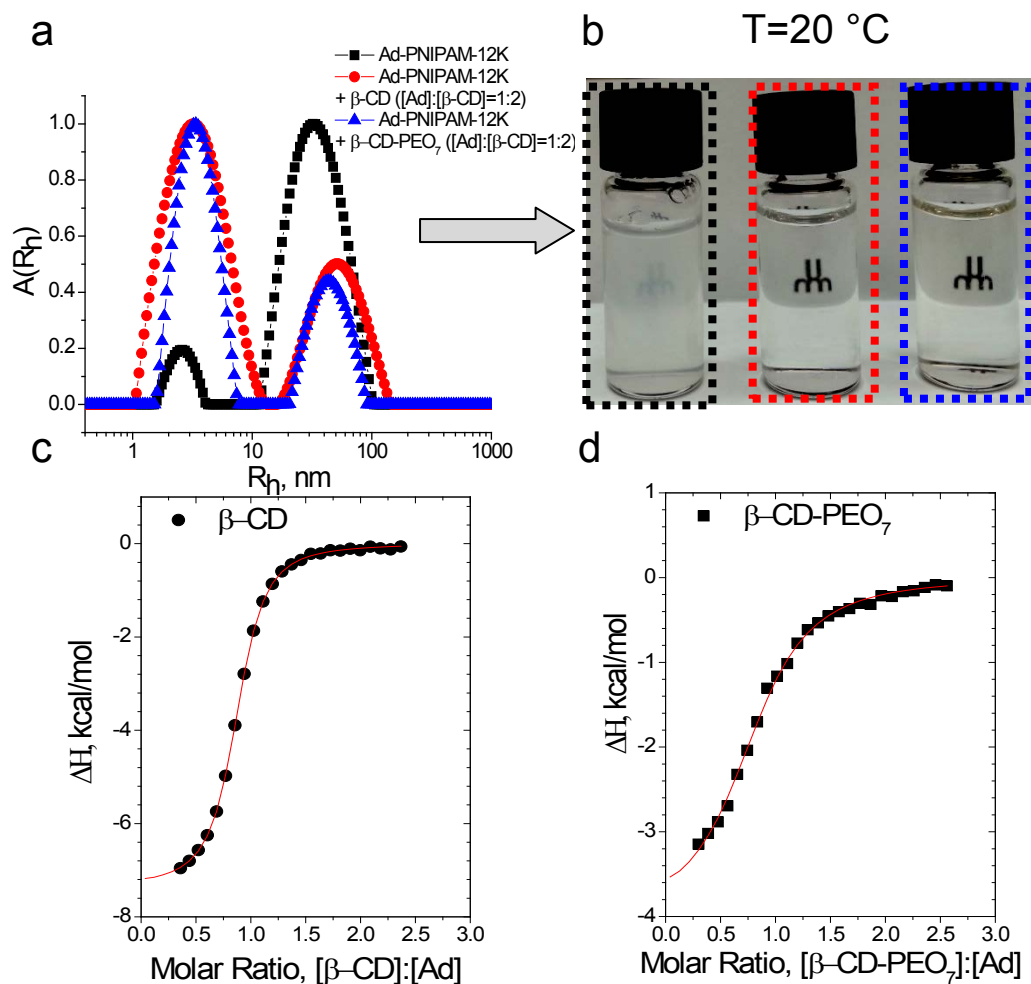
Figure 5: (a) DLS plot of aqueous solutions of Ad-PNIPAM-12K (2 g/L) without and with β-CD or β-CD-PEO$_7$; (b) photos of 5.0 g/L solutions of Ad-PNIPAM-12K (left vial), Ad-PNIPAM-12K in the presence of β-CD (central vial) and in the presence of β-CD-PEO$_7$ (right vial) at 20 °C. Binding enthalpy from the titration of (c) β-CD (4.1 g/L) into Ad-PNIPAM-12K (2.0 g/L) and (d) β-CD-PEO$_7$ (22.0 g/L) into Ad-PNIPAM-12K (2.0 g/L) after subtracting the enthalpy of dilution of β-CD (2.0 g/L) and β-CD-PEO$_7$ (22.0 g/L) into water.
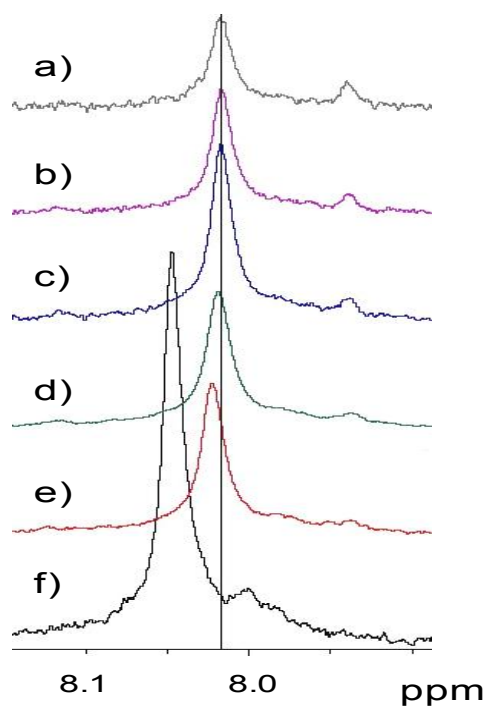
Figure 6: Zoom of the ^{1}H NMR spectrum of polymers mixture (Fig 8.a to 8.e) and of single β-CD-PEO$_7$ (Fig 8.f) in D$_2$O at 23°C: r = [CD]/[Ad] ; a) r = 0.25; b) r = 0.5; c) r = 0.75; d) r = 1; e) r = 1.25; [Ad-PNIPAM-12K] = 2.50.10^{-3} mol/L for a) to e) and [β-CD-PEO$_7$] = 5.00.10^{-3} mol/L for f).
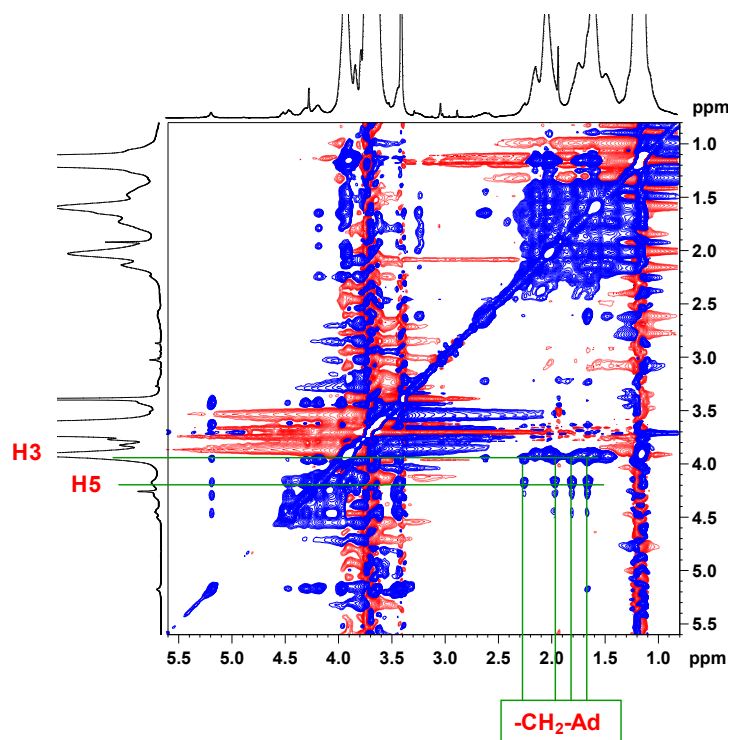
Figure 7: NOESY spectrum of the Ad-PNIPAM-12K /β-CD-PEO$_7$ complex in D$_2$O at 23°C. Experiment with water suppression. [Ad-PNIPAM-12K]=0.5×[β-CD-PEO$_7$]=3.125×10^{-4} mol/L
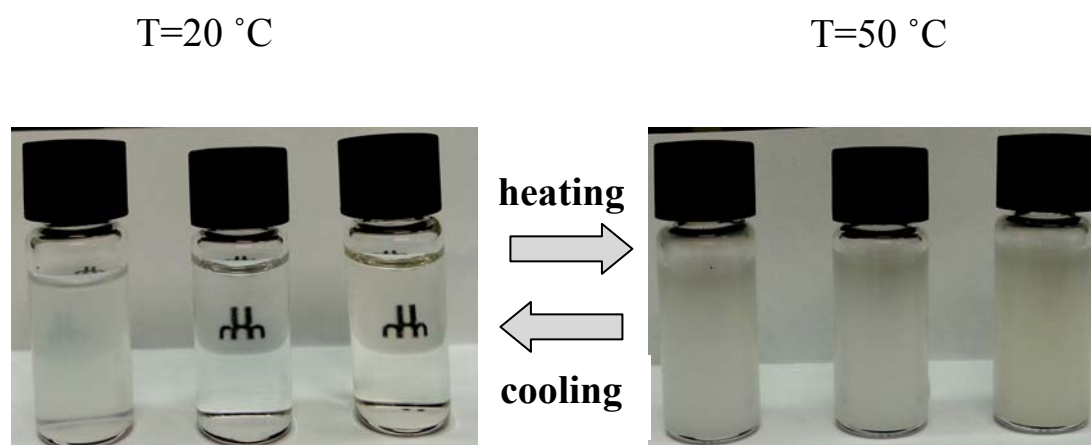

Figure 8. Photos of 5 g/L solutions of Ad-PNIPAM-12K (left vial), Ad-PNIPAM-12K in the presence of β-CD (central vial) and in the presence of β-CD-PEO$_7$ (right vial) at 20 °C or 50 °C.

Ad-PNIPAM-12k

$D=6.15*10^{-8}$ cm^2/sec
$R_h= 73$ nm

$R_g= 55$ nm

Ad-PNIPAM-12k
& β–CD

$D=6.31*10^{-8}$ cm^2/sec
$R_h= 71$ nm

$R_g= 46$ nm

Ad-PNIPAM-12k
& β–CD-PEG$_7$

$D=5.79*10^{-8}$ cm^2/sec
$R_h= 78$ nm

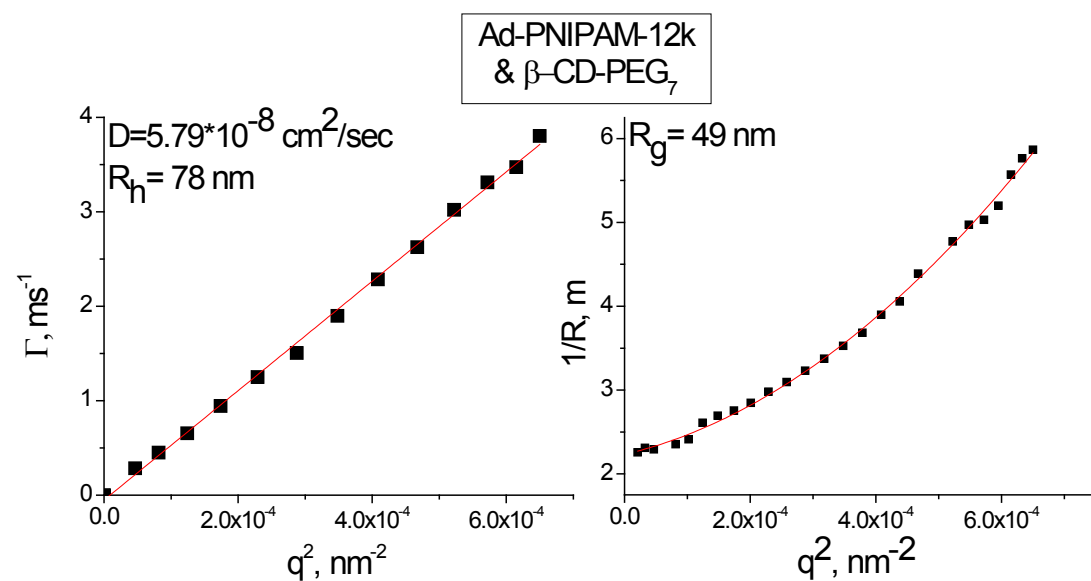$R_g= 49$ nm
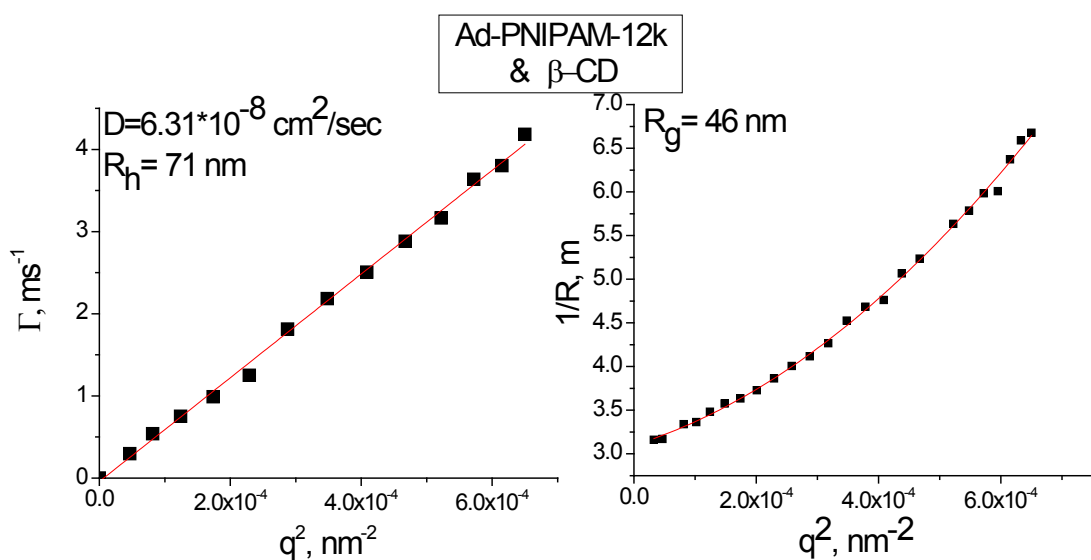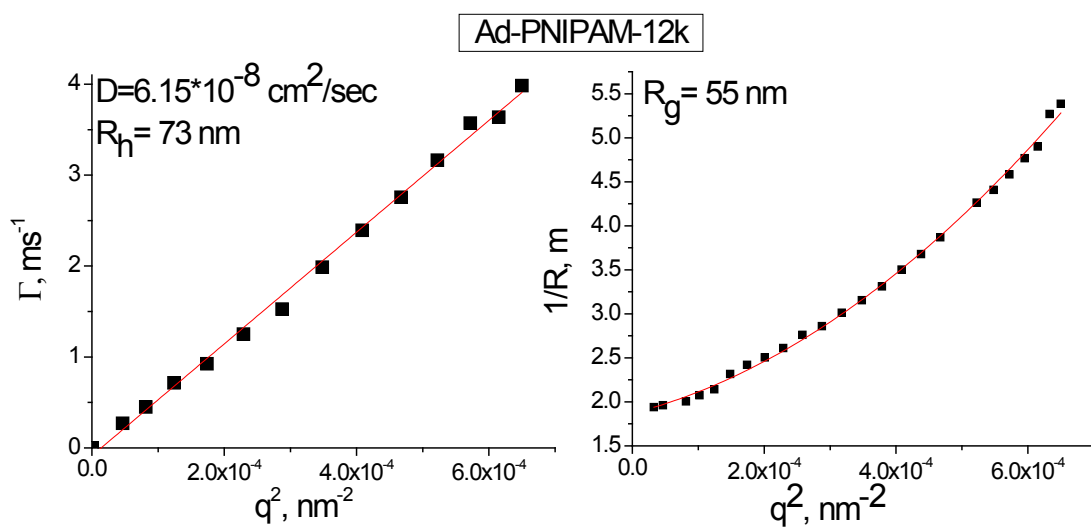
Soft Matter Accepted Manuscript

Figure 9: Determination of hydrodynamic radius R_h and radius of gyration R_g from DLS and SLS measurements, correspondingly. Molar ratio β-CD:Ad=2:1. Concentration of the solution is 0.02 g/L and temperature is 52°C.
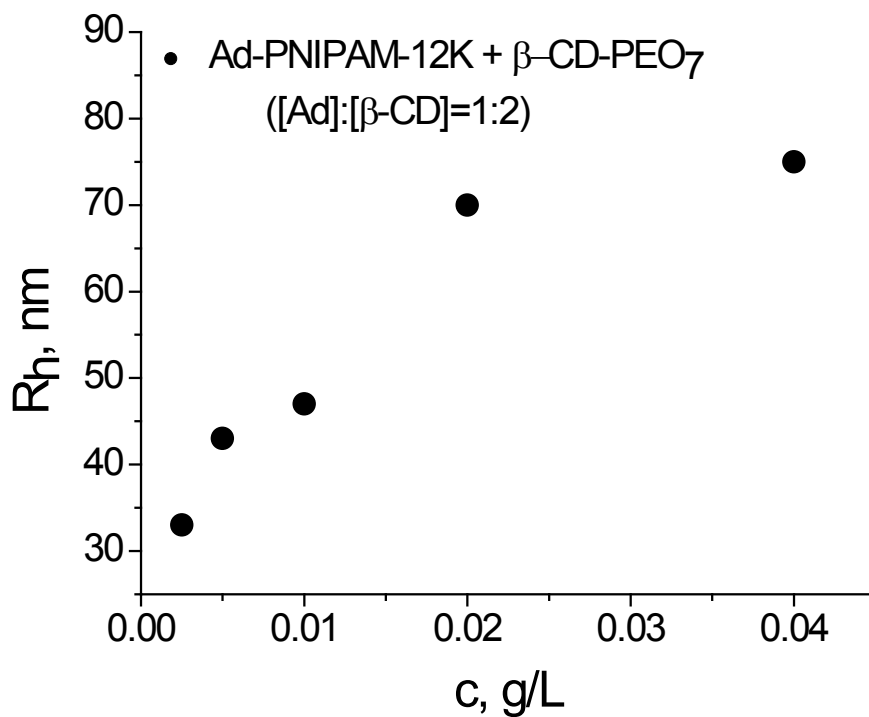

Figure 10. Concentration dependence of the hydrodynamic radius of Ad-PNIPAM-12K the presence of β-CD-PEO$_7$. Molar ratio [β-CD]:[Ad]=2:1. Temperature is 52 °C.

Samples	polymer	Concentration in mol/L	D in m^2/s	
			T=23°C	T=39°C
complex	β-CD-PEO$_7$	6.26×10^{-4}	$7.6 \times 10^{-11} \pm 0.4$	$1.6 \times 10^{-10} \pm 0.06$
	Ad-PNIPAM-12K	3.13×10^{-4}	$6.1 \times 10^{-11} \pm 0.5$	7.7×10^{-11}
Single polymer	β-CD-PEO$_7$	6.26×10^{-4}	$1.2 \times 10^{-10} \pm 0.1$	$1.7 \times 10^{-10} \pm 0.04$
Single polymer	Ad-PNIPAM-12K	3.13×10^{-4}	$6.8 \times 10^{-11} \pm 0.02$	nd

Table 1: DOSY NMR experiments in D$_2$O: determination of the diffusion coefficients of different samples.